RSC Advances

ROYAL SOCIETY OF CHEMISTRY

www.rsc.org/advances

RSC Advances

ARTICLE

Folate-conjugated nanodiamond for tumor-targeted drug delivery

Yu Dong[#a], Ruixia Cao[#a], Yingqi Li[a, b,*], Zhiqin Wang[a], Lin Li[b] and Lu Tian[a]

Received 00th January 20xx,
Accepted 00th January 20xx

DOI: 10.1039/x0xx00000x

www.rsc.org/

An effective drug delivery system based on the functionalized nanodiamond (ND) is constructed by layer-by-layer synthesis. Above all, ND is modified by PEG-diamine and conjugated with folate(FA) to obtain a ND-PEG-FA (NPF) nanocarrier. Then doxorubicin (DOX) is physically attached to the NPF nanocarriers to prepare the drug system (ND-PEG-FA/DOX, NPFD), which exhibits excellent stability under neutral pH conditions, while greatly releases DOX at acidic extracellular fluids (pH 6.5 or pH 5.5). Relying on the role of folate and folate receptor, NPFD nanoparticles tend to discriminate between tumor cells and normal cells and enter the cells by clathrin-dependent and receptor-mediated endocytosis. Interestingly, MTT assay found that NPFD nanoparticles not only played a slow and sustained drug release profile, but also had a tumor-targeted toxicity. This implies that the NPFD system has a capability of targeted drug delivery and can be acted as a nanodrug with promising chemotherapeutic efficacy and safety.

Chemotherapy is one method of treating the tumor diseases, but its biggest drawback is without selective recognition to the tumor cells and the normal cells, which leads to serious side effects to patients in the process of the tumor treatment. With the development of nanotechnology, in the treatment of tumor diseases, drugs conjugated or adsorbed onto the nanocarriers in compared with the free drug having many advantages, such as controlled drug release, altered drug biodistribution, prolonged drug blood circulation, and anti-multidrug resistance, etc. have become a hot research topic.[1,2] A strategy for the tumor-targeted therapy involves the use of a homing ligand, which specifically binds to receptors expressed primarily on the malignant cells. When linked to a therapeutic drug, this ligand can be exploited to carry the nonselective drug specifically into the cancer cells. Such a result can avoid damaging the normal tissues and enhance therapeutic effects. Nanoparticles themselves have a tendency to accumulate in the tumors tissue through the enhanced permeability and retention (EPR) effect,[3] which can achieve passive targeting. However, greater gains, in particular extravasation and tissue penetration, can be achieved by including targeting ligands on the surface of nanoparticles resulting in active targeting to receptors. Based on the fact, with the development of nanotechnology, the applications of nanomaterials functionalized with the appropriate ligands for targeted drug delivery have attracted widespread interests. For example, folate (FA) is a ligand suitable for such conjugation, as folate receptors are often overexpressed on human tumor cells.[4] Moreover, the ligand has relatively simple and well easy conjugation reaction. The simplicity has led to studies of a wide range of folate–nanoparticle conjugates including superparamagnetic nanoparticles,[5,6] gold nanoparticles,[7,8] carbon nanotubes.[9,10]

Since PEG can improve biological properties including high biocompatibility and the weak interactions between PEG and protein, cell and immunogenic, PEG has been used extensively for the administration of biological molecules such as proteins, enzymes, oligonucleotides, and growth factors.[11,12] Furthermore, PEG has been successfully integrated with a variety of nanoparticles such as quantum dots, gold nanoparticles and nanodiamond to enhance their solubility, permeability and stability, simultaneously avoid their quick recognition and elimination by the immune system, and thus prolong the circulation in the body.[13-15]

In recent years, due to the nanodiamonds in all derivatives of carbon nanomaterials having the lowest toxicity, high biocompatibility, and easy surface modification, etc., so the current research on nanodiamonds has attracted wide attention. With the development of nanotechnology, the application of nanodiamonds for drugs delivery was increasing. For example, nanodiamonds have been shown to load different chemotherapy drugs[16-21] and have high

[a] *Department of Chemistry, College of Chemistry and Chemical Engineering, Shanxi University, Taiyuan 030006, PR China.*
[b] *Key Laboratory of Chemical Biology and Molecular Engineering of Ministry of Education, Institute of Molecular Science, Shanxi University, Taiyuan 030006, PR China*
[#] Yu Dong, Ruixia Cao：Co-authors
* E-mail: wkyqli@sxu.edu.cn
Electronic Supplementary Information (ESI) available: [details of any supplementary information available should be included here]. See DOI: 10.1039/x0xx00000x

biocompatibility proved through a variety of *in vitro* and *in vivo* experiments.[22-25]

To continue to open up the application of nanodiamonds in the biological field, in the present work, PEGlated nanodiamond was conjugated with the folate (ND-PEG-FA, NPF), and then doxorubicin hydrochloride (DOX), a chemotherapy drug, was physically adsorbed onto the NPF to obtain the ND-PEG-FA/DOX (NPFD) nanoparticles. The release behavior of doxorubicin *in vitro* and the cellular biological effect was investigated, which gives a platform for drug delivery and targeted therapy to cancer cells.

The preparation of ND-PEG-FA/DOX (NPFD) was displayed in scheme 1. Since doxorubicin is a weak base with a pK_b of 8.3, doxorubicin in sodium borate buffer solution with a pH of 8.0 would result in ionized

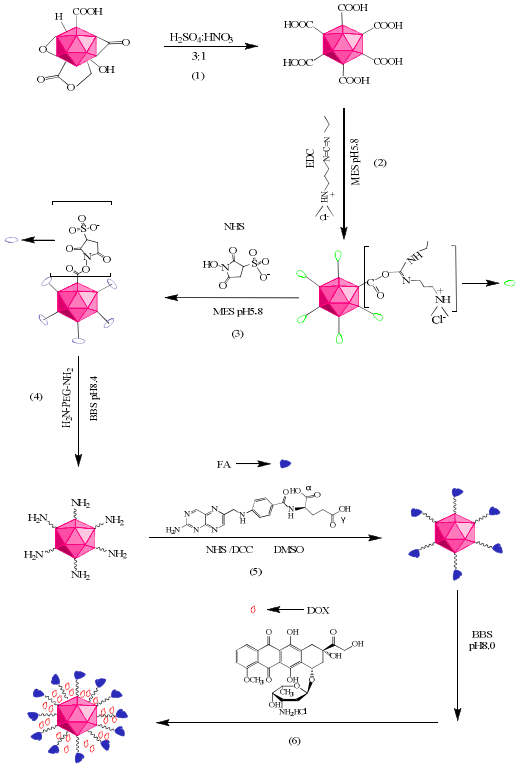

Scheme 1. The ND-PEG-FA/DOX formulation.

NH_3^+ and would associate with α-COO^- on the ND-PEG-FA via electrostatic interaction. Besides, the ND-PEG-FA/DOX complexes may be the result of hydrogen bonding, and Van der Waals forces between doxorubicin molecules and groups on ND-PEG-FA. In addition, a π⋯π interaction has to be considered as a result of the presence of delocalized π bond for two molecules. In the system, the amount of PEG and FA conjugated was (200±15) μg mg^{-1} (Fig. S1) and (44±6) μg mg^{-1} (Fig. S2), respectively. The order of magnitude for FA coupling was about 10 times as much as the previously reported.[26]

In order to improve the amount of drug loaded onto ND-PEG-FA nanoparticles, firstly, the adsorption of DOX onto ND-PEG-FA vector with time was explored to obtain the absorption curve shown in Fig.1A. One can see that there exists a dynamic equilibrium process of the adsorption and dissociation between DOX and ND-PEG-FA, which contains two kinetic behaviors: (1) within three hours, the dissociation rate accounts for the main control position, resulting in the amount of DOX adsorbed on nanoparticles decreasing with time, in line with zero-order kinetics behavior; (2) within 3-5 hours, the adsorption rate is greater than the dissociation rate, resulting in the amount of DOX adsorbed on nanoparticles increasing with time, but after five hours, the dynamic equilibrium process was occurred between dissociation and adsorption, so the amount of drug adsorbed on nanoparticles has been changed no longer. This behavior follows a first-order kinetics.

Secondly, based on the above experiment, the time of the interaction between DOX and the NPF

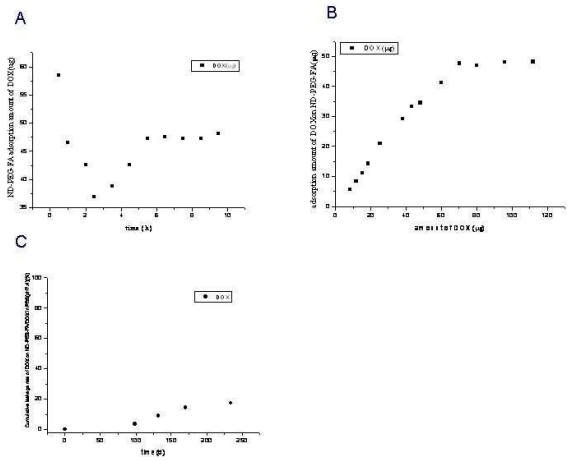

Fig. 1. Optimal conditions for preparing the NPFD system and its stability. (A) Determination of the best time for adsorption of DOX onto ND-PEG-FA nanoparticles; (B) Determination of the maximum amount of adsorption of DOX onto ND-PEG-FA nanoparticles; (C) The stability of the NPFD system in pH 7.4 PBS with time.

nanoparticles was selected as 6 h. The adsorption curve of DOX onto the NPF nanoparticles was shown in Fig.1B. The result showed that the amount of DOX adsorbed was increasing with the increasing DOX quality, until a saturation platform was reached at about 47μg per milligram NPF and then the absorption amount leveled off. The adsorption of DOX onto the NPF nanoparticles fitted the Langmuir adsorption isotherm,[17] calculated the NPFD adsorption constant being K_a = (7.57±0.72)×10^6 M^{-1}, which was near 7 times than that of ND-DOX K_a = (1.13±0.06)×10^6 M^{-1}.[19] It indicated that the NPFD nanodrug had higher stability than the ND-DOX nanodrug.

In fact, the stability determined for NPFD nanoparticles illustrated that it had a high stability (Fig. 1C), where the NPFD nanoparticles were allowed to be stood at 4 °C and pH 7.4 PBS medium for about 250 days to find the DOX leakage rate of less than 20%.

The formation of ND-PEG-NH_2 and ND-PEG-FA/DOX was confirmed further by Fourier transform infrared (FTIR) analysis. The FTIR peaks, indicated with the arrows in Fig.2A(c), Fig.2B(e) and Fig.2C(g), can be clearly assigned to the couple of PEG and FA, the adsorbed DOX, respectively. As a comparison, the FTIR spectrum for pure PEG,

FA, DOX and carboxylated ND are shown in Fig.2. In addition to the readily formed aqueous ND suspensions, the nature of the ND can be seen in the rich presence of functional -OH and –COOH groups in the FTIR spectrum, as shown in Fig.2A(a).

EDS mapping of the elemental analysis for NPFD and distribution of nitrogen on the pristine diamond sheets were obtained from STEM, as shown in Fig.3. From Fig.3A, it can be seen that the distribution of carbon and nitrogen elements is basically the same as nanodiamond frame in

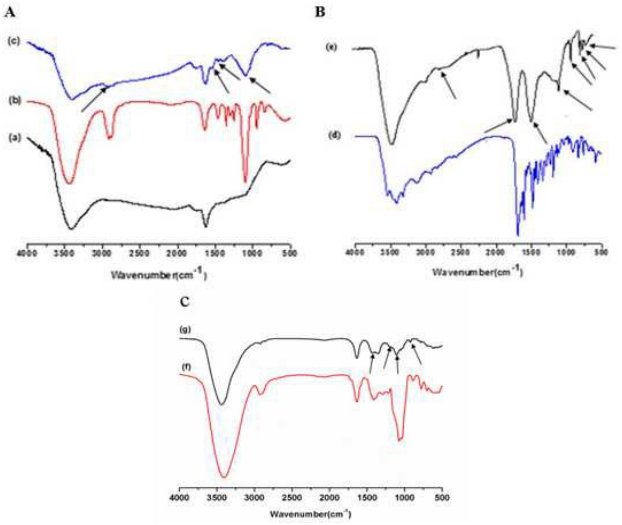

Fig. 2. The FTIR spectrum of various materials. A (a) ND; (b) NH_2-PEG-NH_2; (c) ND-PEG-NH_2. B (d) FA; (e) ND-PEG-FA. C (f) DOX; (g) ND-PEG-FA/DOX.

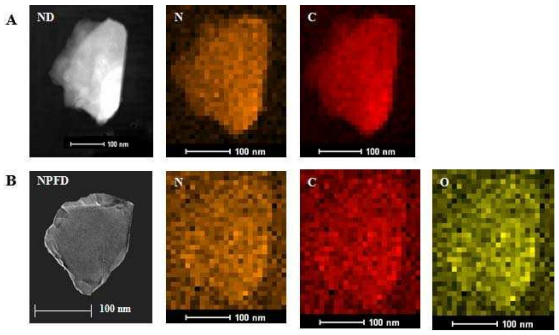

Fig. 3. EDS mapping of pristine ND and NDFD nanoparticles from STEM. (A) The distribution of carbon and nitrogen elements in pristine ND. (B)The distribution of carbon, nitrogen and oxygen elements in NPFD nanoparticle.

Table 1 Average size and zeta potentials for different nanoparticles

Nanoparticles	Diameter (nm)	Zeta Potentials (mV)
ND	156.8±5.5	- 35.0±3.8
ND-PEG-NH_2	187.62±4.85	-22.17±1.42
ND-PEG-FA	201.96±6.23	-26.92±2.53
ND-PEG-FA/DOX	232.47±5.21	-24.35±3.46

pristine nanodiamond, but in NPFD nanoparticle as shown in Fig.3B, the distribution of carbon and nitrogen elements has exceeded nanodiamond frame structure. Furthermore, the distributions of oxygen element was also detected, which showed a similar phenomenon. So the method proves once again that coating of on the diamond sheets has been formed and implies size of NPFD becomes large in compared to pristine ND.

In addition, Dynamic light scattering was used to determine the average size and zeta potential of the ND, intermediate and NPFD as shown in Table 1. Compared with pristine ND, an average size of the nanoparticles by layer-by-layer synthesis were increased, and zeta potentials were changed accordingly, which was indicative of surface binding.

It is well known that efficient drug released from a carrier system is a prerequisite for therapeutic activity of most macromolecular anticancer conjugates. Incorporation of acid sensitivity between the drug and carrier enables the release of an active drug from the carrier into the tumor tissue, either in slightly acidic extracellular fluids (a tumor environment, pH 6.5) or after endocytosis in the endosomes (pH 5–6) or lysosomes (pH 4–5) of the cells.[27-28] For these reasons, the drug release behavior of NPFD was investigated under a simulated physiological condition (phosphate-buffered saline, pH 7.4) and acidic environments (phosphate-buffered saline, pH 5.5, an acidic endosome environment and pH 6.5, a

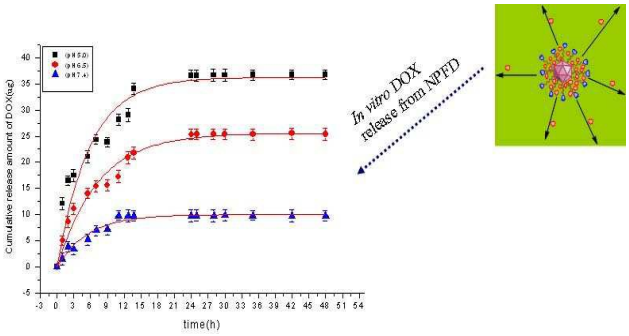

Fig.4. Cumulative release of DOX from NPFD nanoparticles in different pH (PBS, pH 5.0 (■), 6.5(●), 7.4(▲)) with time *in vitro*.

simulated tumor environment) at 37 °C to assess the feasibility of NPFD as an anticancer drug delivery system. As shown in Fig. 4, the rate and amount of DOX released from NPFD were dependent on the pH. NPFD displayed a more release of DOX at pH 5.5 and pH 6.5 than at pH 7.4. At pH 5.5 and pH 6.5, NPFD released about 35% and 23% of DOX, respectively; however, at pH 7.4, NPFD released only 7% of DOX even if NPFD release lasted 50 hours. These results indicated that the amount of DOX released from NPFD was governed by an acidic environment. A small amount of DOX dissociated slowly at pH 7.4, which mimiced the physiological environment of the bloodstream, ensured that minimum amount of DOX was released in the circulation to lead to low side effects.

Due to the fact that side scatter (SS) by flow cytometry analysis can indicate the particle complexities within the cells, the cellular

uptake of NPFD can be indirectly demonstrated by SS. Fig. 5A showed that the data of SS increased for HepG2 cells treated with NPFD compared to cells alone. It suggested that NPFD nanoparticles indeed entered the cells, and as was also confirmed by the images in Fig. 5D(a). In addition, with the increase of concentration or prolonged exposure time, NPFD exhibits higher uptake, suggesting an obvious dose- and exposure duration-dependent manner (Fig. S3).

It has previously reported that ND-PEG-FA nanoparticles are a FR-mediated uptake process.[26] Then whether NPFD nanoparticles are like that to enter the cells.[26] To confirm this speculation, a competitive inhibition assay was performed. In this assay, the HepG2 cells were incubated with the particles either with or without free FA in the medium. Not surprisingly, the uptake of NPFD was effectively suppressed by addition of free FA in a dose-dependent manner (Fig. 5B). While free FA was 1.5 mM, the inhibition ratio obtained was nearly 65%. Such a distinct suppression effect showed that the internalization of the folate-conjugated nanoparticles was hindered due to the reduced availability of FA on the cell surface. It supported the notion that the NPFD nanoparticles were able to specifically target their receptors on cells. In Fig. 5D, we also compared the fluorescence images of HepG2 cells incubated with NPFD without (Fig. 5D(a)) or with (Fig. 5D(b)) free FA in DMEM with 10% FBS. As one can seen, the amount of NPFD internalized drastically reduced when the HepG2 cells were pretreated with free FA. This observation was in line with the results of the flow cytometry analysis (Fig.5B).

To further confirm that the cellular uptake of NPFD was a targeting effect, HEK293 (low-expressed FR) cells were also used as controls compared to HepG2 cells (over-expressed FR). As the results of the flow cytometry analysis, it can be found that the amount of NPFD

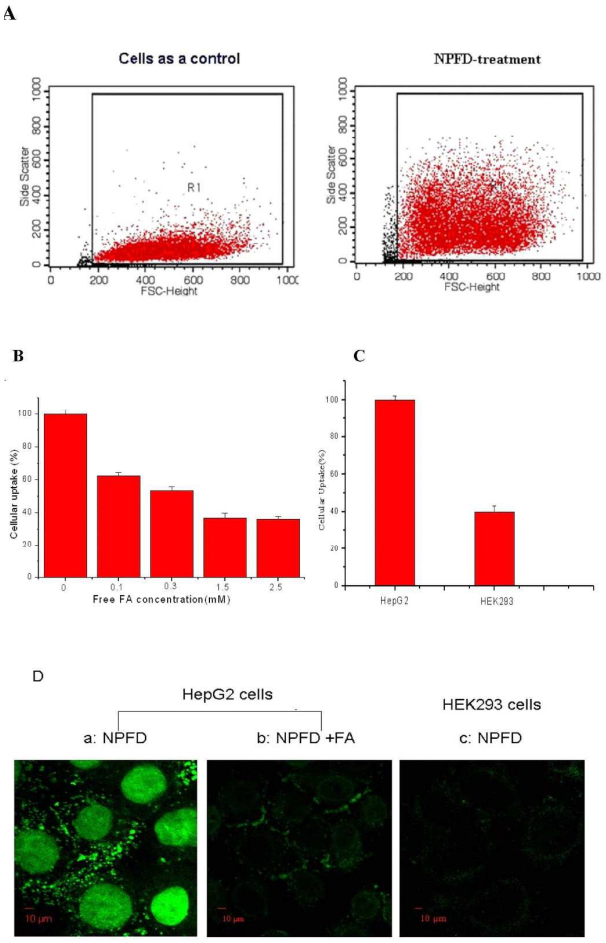

Fig. 5. The uptake of NPFD by HepG2 cells or HEK293 cells. (A) The particle complexity was quantified from a minimum of 10,000 cells by Cell Quest software using flow cytometry analysis. (B) Dependence of the uptake of NPFD by HepG2 cells on the concentration of free FA in DMEM with 10% FBS. (C) The cellular uptake analysis for NDFP nanoparticles in HepG2 and HEK293 cells by flow cytometry analysis. (D) The endocytosis of nanoparticles was observed by the confocal microscope. (a) The images of HepG2 and (c) HEK293 cells treated with NPFD nanoparticles (b) Cells was saturated with free FA in culture media for 0.5 h before treatment with NPFD nanoparticles. The green fluorescent signals were from DOX adsorbed onto the ND-PEG-FA nanoparticles.

internalized by HEK293 cells significantly reduced compared with that of HepG2 cells-treated (Fig. 5C). The endocytosis ratio for the HEK293 cells was 40% of that by HepG2 cells under the same conditions as shown in Fig.5C, which is mainly due to over-expressed folate receptors on the surface of HepG2 cells to induce NPFD high affinity to the cells in compared with the HEK293 cell with low-expressed folate receptors. Thus, NPFD can discriminate between tumor cells and normal cells. In Fig. 5D, we also compared the fluorescence images of HepG2 and HEK293 cells incubated with NPFD in DMEM with 10% FBS, and the amount of NPFD internalized by HEK293 cells (Fig. 5D(c)) markedly reduced compared with that of HepG2 cells (Fig. 5D(a)). It was cons*istent* with the results of the flow cytometry analysis. So FA receptors played an important role in the endocytosis process of NPFD. Furthermore, whether the

uptake of NPFD is energy and clathrin-dependent, the experiment was also carried out and the outcome revealed that the uptake of NPFD was an energy and clathrin-dependent process (Fig. S4). A conclusion can be drawn that the pathway for NPFD entering cells was a clathrin-dependent and FR-mediated endocytosis.

The viability of the HepG2 cells treated by the NPFD nanoparticles with time and concentration was evaluated by using an MTT assay to determine the effect on cell proliferation, where free DOX acted as a control. The cytotoxicity behaved time-dependent. No significant differences in the proliferation of the cells were observed in the presence of both ND-PEG and ND-PEG-FA nanoparticles (Fig. 6A), which indicated the excellent biocompatibility. In Fig. 6A, cells-treated by free DOX exhibited the severest cytotoxicity compared with cells-treated by the NPFD nanoparticles. Interestingly, with time increasing, the lethal level of NPFD nanoparticles to cells was consistent with that of free DOX-treated cells in 100 h. The result strongly pointed that NPFD nanoparticles not only played a slow and sustained drug release profile, but also had a good therapeutic effect. In addition, the cytotoxicity had concentration-dependent for the NPFD nanoparticles for 48h as demonstrated in Fig.6B. The difference in cytotoxicity between DOX alone and NPFD nanoparticlesis was mainly attributable to a slow and sustained drug release capability for the latter.

Moreover, the effects of ND, ND-PEG, ND-PEG-FA, DOX and NPFD on cellular proliferation and morphologies were also investigated. Here the cells were treated either with DOX or NPFD for 50 and 100 h, respectively, which was shown in Fig.6C.Extensive cells death was induced in the presence of DOX, which significantly decreased the cell number, and abnormal morphology of the remaining debris was also observed (Fig. 6C, (b)-(c)). There was reduction in the cell number and the remaining debris observed with NPFD (Fig. 6C, (b)-(c)), but the number of the cells for the latter was greater than that of the former. As a control experiment, the cells cultured in ND, ND-PEG or ND-PEG-FA nanoparticles only resulted in standard cell morphologies and density/viability (Fig. 6C, (a)), which was indicative of healthy growth. The results again implied that the NPFD composites were active and possessed slow and sustained drug release capabilities.

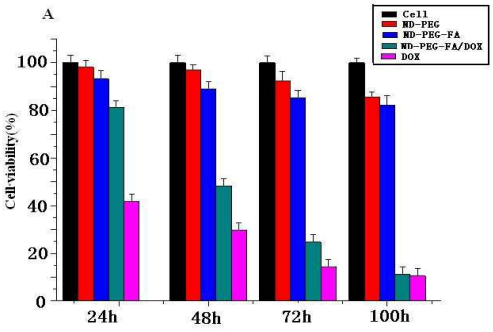

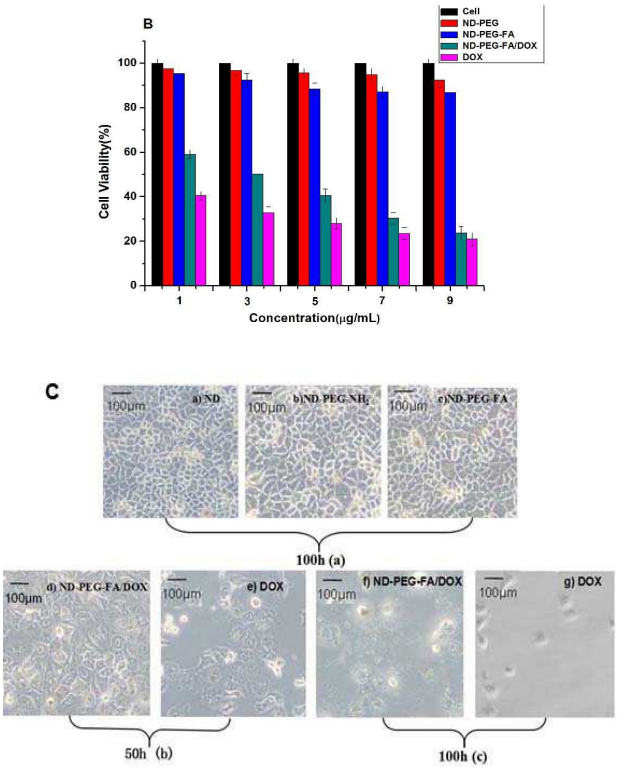

Fig.6. Effect of ND-PEG, ND-PEG-FA and DOX and NPFD on HepG2 cell growth. MTT assay results showing the time (A) and concentration (B)-dependent effects of ND, ND-PEG-FA and DOX and NPFD on cell viability. Five replicates were performed for each treatment. (C) Cell morphological changes were observed by microscope with different nanoparticles. (a) Cells culture with NDs (106 μg mL^{-1}), ND-PEG-NH_2 (106 μg mL^{-1}), ND-PEG-FA (106 μg mL^{-1}) for 100 h, respectively; (b) Cells culture with ND-PEG-FA/DOX (106 μg mL^{-1} NDs＋5 μg mL^{-1} DOX) and DOX (5μg mL^{-1} DOX) for 50 h, respectively; (c) Cells culture with ND-PEG-FA/DOX (106 μg mL^{-1} NDs＋5μg mL^{-1} DOX) and DOX (5 μg mL^{-1} DOX) for 100 h, respectively. (scale bars:100 μm).

Furthermore, MTT assay also showed that NPFD had a targeting function (Fig. S5). Three tumor cell lines (HeLa, HepG2, and C6) with different over-expressed FR on the cell surface were dosed with NPFD nanoparticles at a particle concentration containing DOX 5 μg mL^{-1} for 24 h at 37 °C. Flow cytometry was performed to quantify the cytotoxicity. As shown in Fig. S5, all the cancer cells treated with NPFD nanoparticles in this study showed cytotoxicity after 24 h. The toxicity clearly followed the trend of HeLa＞C6＞HepG2, which correlates well to the FR expression level on these cell lines.[29-31]

Conclusions

In this study, surface modification of nanodiamond was done with PEG and folate. Then DOX was attached to ND-PEG-FA nanocarriers, which has outstanding biocompatibility and high adsorption capacity. The drug release profile showed that NPFD nanoparticles have excellent stability under neutral pH conditions, while greatly releases DOX at acidic extracellular fluids (pH 6.5 or pH 5.5). MTT assay found that NPFD nanoparticles not only played a slow and sustained drug release profile, but also had a good therapeutic effect. More

importantly, with the help of the interaction between FA and FA receptor, NPFD nanoparticles tend to selectively attach onto tumor cells rather than normal cells and enter the cells by clathrin-dependent and receptor-mediated endocytosis. Interestingly, the cytotoxicity clearly followed the trend of HeLa＞C6＞HepG2, which correlates well to the FR expression level on these cell lines. The further study displayed that the cellular uptake of NPFD was in time, energy, dose-dependent process. In addition, the NPFD nanoparticles located in the cytoplasm and DOX was released from NPFD nanoparticles under certain conditions, then DOX could enter the nucleolus playing a role in inhibiting tumor growth by a laser scanning confocal microscope. Therefore, NPFD is a promising anticancer drug, and this can greatly improve anti-tumor effect and reduce potential side effects.

Acknowledgements

This work is supported by the National Natural Science Foundation of China (Grant No. 21071091), Shanxi Science and Technology Development Program (Grant No.20130313021-1).

Notes and references

1 J. A. Barreto, W. O. Malley, M. Kubeil, B. Graham, H. Stephan and L. Spiccia, Adv. Mater., 2011, **23**, H18.
2 H. Gong, L. Cheng, J. Xiang, H. Xu, L. Feng, X. Shi and Z. Liu, Adv. Funct. Mater., 2013, **9**, 48.
3 Y. Matsumura and H. Maeda, Cancer Res., 1986, **46**, 6387.
4 J. Sudimack and R. J. Lee, Adv. Drug Deliv. Rev., 2000, **41**, 147.
5 J. Zhang, S. Rana, R. S. Srivastava and R. D. Misra, *Acta Biomater*., 2008, **4**, 40.
6 M. K. Yoo, I. K. Park, H. T. Lim, S. J. Lee, H. L. Jiang, Y. K. Kim, Y. J. Choi, M. H. Cho and C. S. Cho, *Acta Biomater.*, 2012, **8**, 3005.
7 G. A. Mansoori, K. S. Brandenburg and A. Shakeri-Zadeh, *Cancers* 2010, **2**, 1911.
8 A. Mehdizadeh, S. Pandesh, A. Shakeri-Zadeh, S. K. Kamrava M. Habib-Agahi, M. Farhadi, M. Pishghadam, A. Ahmadi, S. Arami and Y. Fedutik, *Lasers Med Sci.*, 2014, **29**, 939.
9 N. M. Dinan, F. Atyabi, M. R. Rouini, M. Amini, A. A. Golabchifar and R. Dinarvand, *Materials Science and Engineering C*, 2014, **39**, 47.
10 L. Niu, L. J. Meng and Q. H. Lu, *Macromol. Biosci.*, 2013, **13**, 735.
11 A. Adnan, R. Lam, H. N.Chen, J. Lee, D. J. Schaffer, A. S. Barnard, G. C. Schatz, D. Ho and W. K. Liu, *Mol. Pharm*., 2011, **8**, 368.
12 J. Li, Y. Zhu, W. Li, X. Zhang, Y. Peng and Q. Huang, *Biomaterials*, 2010, **31**, 8410.
13 J. P. Ge, H. Lee, L. He, J. Kim, Z. D. LU, H. Kim, J. Goebi, S. H. Kwon and Y. D. Yin, *J. Am. Chem. Soc*., 2009, **131**, 15687.
14 A. Sabnis, A. S. Wadajkar, P. Aswath and K. T. Nguyen, *Nanomed.-Nanotechnol*, 2009, **5**, 305.
15 T. J. Daou, L. Li, P. Reiss, V. Josserand and I. Texier, *Langmuir*, 2009, **25**, 3040.
16 T. B. Toh, D. K. Lee, W. X. Hou, L. N. Abdullah, J. Nguyen, D. Ho and E. K. H. Chow. *Mol. Pharmaceutics*, 2014, **11**, 2683.
17 D. X. Wang, Y. L. Tong, Y. Q. Li, Z. M. Tian, R. X. Cao and B. S. Yang. *Diam*. *Relat*. *Mater*., 2013, **36**, 26.
18 J. Li, Y. Zhu, W. X. Li, X. Y. Zhang, Y. Peng and Q. Huang, *Biomaterials*, 2010, **31**, 8410.
19 Y. Q. Li, X. P. Zhou, D. X. Wang, B. S. Yang and P. Yang, *J. Mater. Chem.*, 2011, **21**, 16406.
20 Y. Q. Li, Y. L. Tong, R. X. Cao, Z. M. Tian, B. S. Yang and P. Yang, *Int. J. Nanomed.*, 2014, **9**, 1065.
21 E. K. Chow, X. Q. Zhang, M. Chen, R. Lam, E. Robinson, H. J. Huang, D. Schaffer, E. Osawa, A. Goga and D. Ho, *Sci. Transl. Med*., 2011, **3**, 73ra21.
22 Y. K. Tzeng, O. Faklaris, B. M. Chang, Y. Kuo, J. H. Hsu and H. C. Chang, *Angew. Chem. Int. Ed.*, 2011, **50**, 2262.
23 Y. J. Fu, N. An, S. H. Zheng, A. H. Liang and Y. Q. Li, *Diam. Relat. Mater.*, 2012, **21**, 73.
24 N. Mohan, C. S. Chen, H. H. Hsieh, Y. C. Wu and H. C. Chang, *Nano Lett*., 2010, **10**, 3692.
25 V. Vaijayanthimala, P. Y. Cheng, S. H. Yeh, K. K. Liu, C. H. Hsiao, J. I. Chao and H. C. Chang, *Biomaterials*, 2012, **33**, 7794.
26 B. L. Zhang, Y. Q. Li, C. Y. Fang, C. C. Chang, C. S. Chen, Y. Y. C and H. C. Chang, *Small*, 2009, **5**, 2716.
27 Y. H. Li, J. Wang, M. G. Wientjes and J. L. S. Au, *Adv. Drug Delivery Rev.*, 2012, **64**, 29.
28 E. S. Lee, Z. G. Gao, and Y. H. Bae, *Journal of Controlled Release, 2008, **132**, 164.*
29 C. Y. Ang, S. Y. Tan, X. L. Wang, Q. Zhang, M. Khan, L. Bai, S. T. Selvan, X. Ma, L. L. Zhu, K. T. Nguyen, N. S. Tan and Y. L. Zhao, *J. Mater. Chem. B,* 2014, **2**, 1879.
30 Y. Hattori and Y. Maitani, *J Control Release*, 2004, **97**, 173.
31 J. E. Schroeder, I. Shweky, H. Shmeeda, U. Banin and A. Gabizon, *J. Control*. *Release*, 2007, **124**, 28.